On the static and dynamical transition in the mean-field Potts glass

1995 J. Phys. A: Math. Gen. 28 3025

(http://iopscience.iop.org/0305-4470/28/11/008)

J. Phys. A: Math. Gen. 28 (1995) 3025–3041. Printed in the UK

On the static and dynamical transition in the mean-field Potts glass

Emilio De Santis†, Giorgio Parisi‡ and Felix Ritort†‡

† Dipartimento di Fisica and INFN, Università di Roma 'Tor Vergata', Viale della Ricerca Scientifica, 00133 Rome, Italy

‡ Dipartimento di Fisica and INFN, Università di Roma 'La Sapienza', P Aldo Moro 2, 00185 Rome, Italy

Received 4 November 1994, in final form 30 March 1995

Abstract. We study the static as well as the glassy or dynamical transition in the mean-field p-state Potts glass. By numerical solution of the saddle-point equations we investigate the static and dynamical transitions for all values of p in the non-perturbative regime $p > 4$. The static and dynamical Edwards–Anderson parameter increase with p logarithmically. This makes the glassy transition temperature lie very close to the static one. We compare the main predictions of the theory with numerical simulations.

1. Introduction

This paper is devoted to the study of the glassy properties of the mean-field Potts glass. Very recently there have been new developments in spin-glass theory concerning frustrated mean-field models without explicit disorder [1–7]. It has been shown that these systems do have a glassy transition temperature below which thermal fluctuations are very small and dynamical relaxations are very slow. Even though these results are not new in the context of disordered systems it is most interesting to know that non-disordered models also share these properties.

The purpose of this paper is to study the glassy behaviour of a disordered spin glass. In general, these systems have a static transition T_{RSB} where replica symmetry is broken. The breaking of the replica symmetry can occur in two ways. There can be a continuous breaking pattern (as happens in the case of the Sherrington–Kirkpatrick (SK) model [8]) or there can be a one-step breaking of the replica symmetry (as happens in p-spin models with $p > 2$ [9]). Also one can find intermediate phases where there is a pattern with one step of breaking superimposed on a region with continuous breaking (as happens in p-spin models or Potts models at low enough temperatures). The breaking pattern is fully described by the order parameter $q(x)$ which is a function defined in the interval $(0, 1)$ [10].

The study of a disordered model with a discontinuous transition in the order parameter is of particular interest. These systems generally have a temperature T_G where a dynamic instability appears. This temperature is called the glass temperature and is higher than the transition T_{RSB} where the replica symmetry breaks. The first observation of this type was due to Kirkpatrick and Thirumalai, who solved the off-equilibrium dynamics for the p-spin model above the glass temperature [11]. Subsequently, Kirkpatrick, Thirumalai and Wolynes studied the Potts mean-field glass, reaching similar conclusions [12, 13]. Similar

0305-4470/95/113025+17$19.50

results were obtained in the case of the p-spin spherical spin glass by Crisanti *et al* [14]. Below the glass transition it has been shown by Cugliandolo and Kurchan [15] that the energy of the p-spin spherical spin-glass model in the low-temperature phase is higher than that predicted by the statics. For times larger than a time scale (which diverges exponentially with the size of the system) it is expected that the energy of the system will relax to its equilibrium value. How fast this time scale grows with the size of the system depends on particular features of the glass transition like the discontinuity in the Edwards–Anderson parameter q_G.

In order to investigate the glassy behaviour of a disordered model we have decided to study the infinite-ranged Potts glass model. The reason is threefold. First, in the Potts model p is a tunning parameter for the magnitude of the static and the dynamical transition. Second, the Potts model is amenable of numerical tests while other models like the p-spin model (Ising or spherical) are time consuming which makes numerical simulations practically impossible for $p > 3$. The situation is different in the case of the random orthogonal model [2] where the replica theory predicts the existence of a glassy phase in good agreement with the numerical simulations. Third, the Potts glass model lacks the reflection symmetry $\sigma_i \to -\sigma_i$ of some other models. This makes it more similar to real structural glasses.

In this paper we completely solve the replica equations for the Potts model for an arbitrary number of states p. We will be able to compute exactly the static and the dynamical transition and we will compare the predictions with numerical simulations.

We will see that a complete dynamical freezing never takes place, even for very large values of p. For generic p there is always a residual entropy at the static transition T_{RSB}. As shown by Gross *et al* [16] in the limit $p \to \infty$ the statics of the Potts model converges to the random energy model (REM) [17,28]. We will see that the convergence of the statics of the Potts glass model to the REM when $p \to \infty$ is very slow (logarithmic in p). Surprisingly, we will see that also the dynamics converges logarithmically with p to a fully frozen dynamics but even more slowly than does the statics. For all practical purposes, i.e. for reasonable values of p, the system is never fully frozen. In addition we will see that, for $p > 4$, the dynamical transition (also called the glass transition) is always very close to the static transition. This makes the glassy behaviour of the Potts model very different from other models with a discontinuous transition in the order parameter like, for instance, the p-spin interaction Ising spin-glass model where the static and the dynamic Edwards–Anderson order parameter increase relatively fast with p.

This partial freezing which occurs for the mean-field Potts glass has to be compared with deterministic models [1,6,5] where $q_G \sim 1$. In those cases there is no quenched disorder and frustration is purely dynamical and self-induced by the dynamical process [3].

The paper is organized as follows. In section 2 we introduce the model and we write closed expressions for the free energy at first order of replica symmetry breaking. In section 3 we solve numerically the static equations at one step of replica symmetry breaking and we determine the static and the dynamical transition. Section 4 compares the predictions with the numerical simulations. Finally we present our conclusions.

2. Static replica equations for the Potts glass

The Potts glass model is defined by the random Hamiltonian

$$\mathcal{H} = -p \sum_{i<j} J_{ij} \delta_{\sigma_i \sigma_j} \tag{1}$$

where p is the number of states and the variables σ can take the values $0, 1, \ldots, p-1$. The sum is extended over all $\frac{1}{2}N(N-1)$ pairs in the lattice and N is the number of sites. The couplings J_{ij} are randomly distributed with mean $\frac{J_0}{N}$ and variance $\frac{1}{N}$. In order to solve this random model we apply the replica method in order to compute the free energy f

$$\beta f = \lim_{n\to 0} \frac{\log \overline{Z_J^n}}{Nn} \tag{2}$$

where n is the number of replicas and the overline means average over the disorder. Performing the usual transformations (avergaging over the disorder, decoupling the sites and introducing auxiliary fields) and using the identity ($a, b = 1, \ldots, n$ are replica indices)

$$\delta_{\sigma_i^a \sigma_j^b} = \sum_{r=0}^{p-1} \delta_{\sigma_i^a r} \delta_{\sigma_j^b r} \tag{3}$$

one gets the following result†

$$\overline{Z_J^n} = \int \mathrm{d}m_a^r \, \mathrm{d}Q_{ab}^{rs} \, \mathrm{e}^{-N A[m,Q]} \tag{4}$$

where $r, s = 0, \ldots, p-1$ denote the Potts states. The function $A[m, Q]$ is given by [19, 20]

$$A[m,Q] = \frac{n\beta^2(1-p)}{4} + \frac{\beta^2}{2p}\left(J_0 + \beta\frac{p-2}{2}\right)\sum_{ar}(m_a^r)^2 + \frac{\beta^2}{2p^2}\sum_{a<b}\sum_{r,s}(Q_{ab}^{rs})^2$$
$$- \log Tr_\sigma \, \mathrm{e}^{H[m,Q]} \tag{5}$$

with

$$H[m,Q] = \frac{\beta}{p}\left(J_0 + \frac{\beta(p-2)}{2}\right)\sum_{a,r} m_a^r (p\delta_{\sigma_a r} - 1)$$
$$+ \frac{\beta^2}{p^2}\sum_{a<b}\sum_{rs} Q_{ab}^{rs}(p\delta_{\sigma_a r} - 1)(p\delta_{\sigma_b s} - 1) \,. \tag{6}$$

The stationary saddle-point equations read

$$\begin{aligned} m_a^r &= \langle p\delta_{\sigma_a r} - 1\rangle \\ Q_{ab}^{rs} &= \langle (p\delta_{\sigma_a r} - 1)(p\delta_{\sigma_b s} - 1)\rangle \end{aligned} \tag{7}$$

where the mean $\langle \cdots \rangle$ is evaluated over the effective Hamiltonian in (6). The order parameters m and Q satisfy the constraints

$$\begin{aligned} \sum_r m_a^r &= 0 \\ \sum_r Q_{ab}^{rs} &= 0 \,. \end{aligned} \tag{8}$$

In the particular case $p = 2$ with $Q_{ab}^{r\neq s} = -Q_{ab}$, $Q_{ab}^{rr} = Q_{ab}$ one recovers the solution for the SK model [8]. It can be shown that ferromagnetic order is always preferred for $p > 2$ for sufficiently low temperatures. The temperature T_F below which ferromagnetic order appears‡ is given by the following condition [20]:

$$\frac{1}{T_F}\left(J_0 + \frac{p-2}{2T_F}\right) = 1 \,. \tag{9}$$

† Alternatively one can use the simplex representation [18].

‡ This transition is from a paramagnet to a collinear ferromagnet.

Even though this formula for T_F is implicit in the formulae of [20] (equation (17) therein) it is not explicitly noted there. In the special case $J_0 = 0$ the ferromagnetic transition appears below $T = 1$ for $p < 4$ and above that temperature for $p > 4$. Our main interest in this paper is the study of the spin-glass transition. In order not to observe the ferromagnetic transition it will be necessary to add an antiferromagnetic coupling in the case $p > 4$. This will be discussed further at the end of this section. The spin-glass solution is given by $m_a^r = 0$. This means that all different p states are equally populated. The saddle-point equations are independent of J_0 and the replica symmetric solution in this case is given by

$$\begin{aligned} Q_{ab}^{r\neq s} &= -q \\ Q_{ab}^{rr} &= q(p-1)\,. \end{aligned} \tag{10}$$

Substituting this result in (7) we obtain

$$\beta f = \frac{\beta^2}{4}(1-p)(1-q)^2 - \int_{-\infty}^{\infty} \prod_{r=1}^{p} \left(\frac{\mathrm{d}y_r}{\sqrt{2\pi}} \mathrm{e}^{-y_r^2/2} \right) \log \left(\sum_{r=1}^{p} \exp(\beta(qp)^{\frac{1}{2}} y_r) \right) . \tag{11}$$

The high-temperature result $q = 0$ gives the free energy f, the internal energy u and the entropy s:

$$\beta f = \frac{\beta^2(1-p)}{4} - \log(p) \qquad u = \frac{\beta(p-1)}{2} \tag{12}$$

$$s = \frac{\beta^2(1-p)}{4} + \log(p)\,. \tag{13}$$

Because the entropy has to be positive one finds that the replica symmetric solution breaks down, at least above or equal to

$$T_0 = \left(\frac{(p-1)}{4\log(p)} \right)^{\frac{1}{2}} . \tag{14}$$

It has been shown [21] that there is a continuous phase transition at $T_c = 1$ for $p < 6$ which is unstable for $p \geqslant 2$. This transition ceases to exist above $p = 6$ and cannot be found within the replica symmetric hypothesis.

It is necessary to break the replica symmetry. By expanding the free energy (5) close to $T_c = 1$, Gross *et al* [16] found two different regimes according to the value of p. In both cases the correct solution is given by one step of breaking. In the region $2.8 < p < 4$ the transition is continuous. The breaking parameter m is $\frac{1}{2}(p-2)$ at the transition temperature $T_c = 1$. At sufficiently low temperatures the entropy of the one-step solution becomes negative and a continuous breaking is then necessary. In the regime $p > 4$ the transition is discontinuous in Q and the breakpoint parameter m is equal to 1 at the transition temperature $T_c > 1$. Cwilich and Kirkpatrick [22] have shown that this one step solution is always stable for $p > p^* = 2.82$ below but close to T_c.

At the first order of replica symmetry breaking we subdivide the n replicas into $\frac{n}{m}$ blocks. Each block contains m replicas [23]. The order parameter Q_{ab}^{rs} takes a certain value when both replicas a, b belong to the same subblock and it is zero when both indices belong to two different subblocks. More explicitly, if K denotes a subblock, we impose

$$\begin{aligned} Q_{ab}^{r\neq s} &= -q \quad (a,b \in K) \qquad Q_{ab}^{r\neq s} = 0 \quad \text{(otherwise)} \\ Q_{ab}^{rr} &= -q(p-1) \quad (a,b \in K) \qquad Q_{ab}^{rr} = 0 \quad \text{(otherwise)}\,. \end{aligned} \tag{15}$$

We obtain the result

$$\beta f = \frac{\beta^2}{4}(1-p) + \frac{\beta^2}{4}(m-1)(p-1)q^2 + \frac{\beta^2}{2}q(p-1) + \frac{\beta^2}{2}qm$$
$$-\frac{1}{m}\log\int_{-\infty}^{\infty}\prod_{r=1}^{p}\left(\frac{dy_r}{\sqrt{2\pi}}e^{-y_r^2/2}\right)\left(\sum_{r=1}^{p}\exp(\beta(qp)^{\frac{1}{2}}y_r)\right)^m . \tag{16}$$

The corresponding saddle-point equations are

$$\frac{\partial f}{\partial q} = \frac{\partial f}{\partial m} = 0 \tag{17}$$

which determine the correct solution. Since we are interested in the glassy behaviour of the Potts model our approach will be to numerically solve the equation (17). This is the purpose of the next section.

Some comments are in order regarding the existence of the ferromagnetic transition. We said previously that the system orders ferromagnetically at sufficiently low temperatures. The temperature T_F below which the system orders ferromagnetically is smaller than 1 for $p < 4$. Also for $p < 4$ the spin-glass transition appears at $T_{RSB} = 1$. This means that in the regime $p < 4$ the spin-glass transition occurs at a temperature T_{RSB} larger than the temperature T_F at which ferromagnetic order sets in. On the other hand, for $p > 4$ the spin-glass transition T_{RSB} occurs at a temperature greater than 1 but smaller than T_F. In order that $T_F < T_{RSB}$ it is necessary to introduce a negative value for J_0. In our numerical simulations we have chosen $J_0 = \frac{1}{2}(4-p)$ in the case $p > 4$ and $J_0 = 0$ for $p < 4$. In this way the spin-glass transition occurs at a larger temperature than the ferromagnetic ordering. Now, let us suppose that we perform a dynamical process of the system in which the temperature is slowly decreased starting from the high-temperature phase. We think that, once the system has entered the metastable glassy phase, then it remains trapped in this phase for a time which diverges exponentially with the size of the system. Consequently, the system is unable to see the ferromagnetic transition which occurs at a lower temperature. This is in agreement with our numerical results where we do not find evidence for strong ferromagnetic ordering when the transition T_{RSB} from a paramagnet to a spin glass occurs at a higher temperature than the ferromagnetic T_F. Only the case $p = 4$ could be a little tricky because the estimate for the ferromagnetic transition T_E and the spin-glass transition coincide, but even in this case we have not observed in the numerical simulations a strong magnetic ordering.

We should note that there are few works devoted to the study of the ferromagnetic behaviour in the mean-field Potts glass and we think it would be very interesting to investigate it.

3. The static and the dynamical transition

In this section we are going to solve (16) numerically. As is usual in spin-glass theory we have to maximize the free energy as a function of q and m. We face the problem of computing the p-dimensional integral

$$I = \int_{-\infty}^{\infty}\prod_{r=1}^{p}\left(\frac{dy_r}{\sqrt{2\pi}}e^{-y_r^2/2}\right)\left(\sum_{r=1}^{p}\exp(\beta(qp)^{\frac{1}{2}}y_r)\right)^m . \tag{18}$$

Because the solution of the replica equations involve a maximization in the (q, m) plane it is essential to compute I with relatively high precision. We have been able to reduce the

p-dimensional integral to a two-dimensional integral. We use the identity,

$$A^{m-1} = \frac{1}{\Gamma(1-m)} \int_0^\infty \mathrm{d}x\, x^{-m} \mathrm{e}^{-Ax} \tag{19}$$

where $\Gamma(x)$ is the Gamma function that is well defined for $x > 0$, i.e. $m < 1$, as is the case once the analytic continuation $n \to 0$ (n is the number of replicas) has been done.

We decompose the integrand in (18) as a product of two terms $A * A^{m-1}$ with A given by

$$A = \sum_{r=1}^{p} \exp(\beta(qp)^{\frac{1}{2}} y_r) \tag{20}$$

Applying (19) and using the fact that the integrand in (18) is invariant under permutation of the indices we get the final result

$$I = \frac{p \exp\left(\frac{1}{2}\beta^2 qp\right)}{\Gamma(1-m)} \int_0^\infty \mathrm{d}x\, x^{-m} (w(x))^{p-1} w\left(x \exp\left(\tfrac{1}{2}\beta^2 qp\right)\right) \tag{21}$$

where $w(x)$ is given by

$$w(x) = \int_{-\infty}^{\infty} \frac{\mathrm{d}y}{\sqrt{2\pi}} \exp\left(-\frac{y^2}{2} - x \exp(\beta(qp)^{\frac{1}{2}} y)\right) \tag{22}$$

The integral over x is well defined and free of divergences. However one has to be careful evaluating the integrand close to $x = 0$. We have been able to maximize the free energy and completely solve the static replica equations up to $p = 40$.

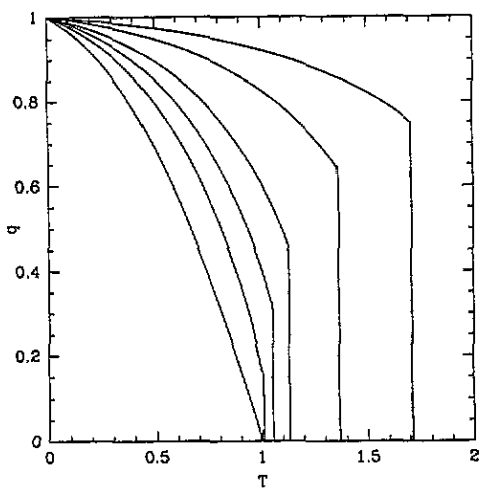

Figure 1. The one-step breaking parameter q as a function of the temperature. From left to right: $p = 3, 5, 7, 10, 20, 40$.

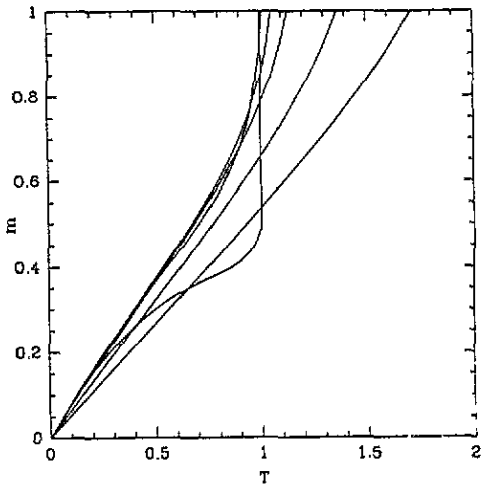

Figure 2. The one-step breaking parameter m as a function of the temperature. The different lines that intersect the upper horizontal axis $m = 1$ correspond from left to right to: $p = 3, 5, 7, 10, 20, 40$.

The results are shown in figures 1 and 2 where we plot the variational parameters q and m as a function of T. We plot the solutions for the cases, $p = 3, 5, 7, 10, 20, 40$. The transition temperature also grows with p. The solution of the integral (21) presents some problems of precision at very low temperatures and also close to the transition temperature,

where it is difficult to determine the value of the discontinuity precisely. A more precise way of computing the critical temperature and the discontinuous jump of q will be presented below. It is interesting to note how slow the convergence to the random energy model is as p increases. When p increases the value of q at the transition point grows very slowly. In fact, in the limit $p \to \infty$, the value of q converges to 1 and the entropy is zero at the transition temperature. Using (14) we obtain that the critical temperature grows as T_0 of (14). This result was already noted in [16].

We have already observed that at very low temperatures the entropy of the one-step solution becomes negative (of order 10^{-2}). Continuous breaking is necessary (as noted in [16]) but we have not studied this type of solution. It is not clear to us if any effect of this new transition could be observable in a numerical simulation.

We now want to show a more precise computation of the critical temperature T_{RSB} and the glass transition T_G. From the dynamical point of view an instability in the dynamical equations appears at a temperature T_G above the static transition T_{RSB} [13]. Using the static approach, this dynamical temperature T_G can be determined computing the smallest eigenvalue in the stability matrix. The vanishing at T_G of this eigenvalue, sometimes called the replicon, corresponds to the marginality condition [26]. In principle, this condition correctly determines the dynamical or glass transition. Anyway it is not clear if it is the correct description of the dynamical behaviour in the low-temperature phase. This condition has been solved numerically in the random orthoghonal model and it has been shown that it correctly describes the dynamical energy below the glass transition for temperatures that are not too low [2]. It also correctly describes the glass transition in the case of deterministic models. The interested reader is referred to [2] for more details. In order to determine the glass transition for the Potts case we should compute the stability matrix of the problem. This is an involved task (which has been done by Cwilich and Kirkpatrick close to T_c [22]) and we will follow a different strategy (already noted by Cwilich and Kirkpatrick but not fully explained). It can be shown that in the limit $m \to 1$ the replicon eigenvalue coincides with the longitudinal eigenvalue. This result can be shown using the exact expressions for the spectrum of the stability matrix which have been reported in the literature at first order of replica symmetry breaking [27]. From the stability analysis results of Cwilich and Kirkpatrick this can also be directly tested in the Potts glass case. Consequently, in order to determine the dynamical transition, it is sufficient to impose the marginality condition for the longitudinal fluctuations.

We expand the free energy (16) around $m = 1$

$$\beta f = \tfrac{1}{4}\beta^2(1-p) - \log(p) + (m-1)\left(\tfrac{1}{4}\beta^2(p-1)q^2 + \tfrac{1}{2}\beta^2 q(p+1) + \log(p) - I_2\right) \tag{23}$$

where the integral I_2 is given by

$$I_2 = \exp\left(-\frac{\beta^2 pq}{2}\right)\int_{-\infty}^{\infty}\prod_{r=1}^{p}\left(\frac{\mathrm{d}y_r}{\sqrt{2\pi}}\mathrm{e}^{-y_r^2/2}\right)\mathrm{e}^{\beta\sqrt{qp}y_1}\log\left(\sum_{r=1}^{p}\exp(\beta(qp)^{\frac{1}{2}}y_r)\right). \tag{24}$$

For $m = 1$ equation (23) reduces to the high-temperature free energy which is independent of q. More generally, we can write the free energy as

$$f = f_0 + (m-1)f_1 + \mathrm{O}\left((m-1)^2\right) \tag{25}$$

where f_0 is independent of q. This general expansion locates the static and the dynamic transition. For the static transition we look for a temperature at which there is a solution

q_{RSB} which satisfies

$$\left(\frac{\partial f}{\partial q}\right)_{q=q_{RSB}} = \left(\frac{\partial f_1}{\partial q}\right)_{q=q_{RSB}} = 0$$
$$(f_1)_{q=q_{RSB}} = 0 \tag{26}$$

For the dynamical transition the stability is marginal and the second derivative of f respect to q vanishes,

$$\left(\frac{\partial f}{\partial q}\right)_{q=q_G} = \left(\frac{\partial f_1}{\partial q}\right)_{q=q_G} = 0$$
$$\left(\frac{\partial^2 f}{\partial q^2}\right)_{q=q_G} = \left(\frac{\partial^2 f_1}{\partial q^2}\right)_{q=q_G} = 0\,. \tag{27}$$

The last equations corresponds to the case where an extremal solution of (23) with $q_G \neq 0$ dissappears. It is then clear that the dynamical transition temperature is always higher than the static one. We have solved these equations for different values of p. Now we face the problem of computing the p-dimensional integral I_2. It can be reduced to a two-dimensional integral using the representation

$$\log(1+A) = \int_0^\infty \frac{dx}{x} e^{-x}(1 - e^{-Ax})\,. \tag{28}$$

and taking

$$A = \left(\sum_{r=1}^{p} \exp(\beta(qp)^{\frac{1}{2}} y_r)\right) - 1 \tag{29}$$

we obtain the result

$$I_2 = \int_0^\infty \frac{dx}{x} e^{-x} \left\{1 - e^x w\left(x \exp(\tfrac{1}{2}\beta^2 qp)\right) w^{p-1}(x)\right\} \tag{30}$$

with the same function w as given in (22). We have solved equations (26) and (27) for different values of p. Our results are summarized in table 1. We find for each value of p two temperatures. One is T_{RSB} and corresponds to the static transition with the discontinuous jump q_{RSB}. The other one is T_G and corresponds to the dynamical transition with the discontinuous jump q_G. Our results for the static transition are in agreement with those found with the previous analysis using the maximization procedure for the free energy. This is a check of our procedures. Moreover, this analysis provides a much more precise determination of the values of q_{RSB}, q_G and the transition temperatures.

The results we have found are also in agreement with those reported by Cwilich and Kirkpatrick, the only difference is that all their computations are perturbative whereas ours are exact. As was obtained in [12] and [22], one finds that $q_G/q_{RSB} = \frac{3}{4}$ for p close to 4. Looking at table 1 the reader can observe that the ratio q_G/q_{RSB} stays so close to 3/4, even for large values of p, that one is tempted to conclude that this is exact at all orders in perturbation theory. Our numerical precision for solving equations (26), (27) is good enough to exclude this possibility. From the results shown in the Table 1 it is clear that convergence to the $p \to \infty$ limit is very slow. Fortunately, our numerical program which solves the equations (26) and (27) is accurate enough to show this slow convergence explicitly even for exponentially large values of p. We have solved the full equations up to $p = 10^6$. The results for q_{RSB} and q_G as a function of $1/\log(p)$ are shown in figure 3.

Furthermore, in the Potts case the ratio T_G/T_{RSB} grows very slowly, with p being always smaller than 1.13 up to $p = 10^6$. The proximity of the temperatures T_G and T_{RSB} makes

Table 1. Solutions to equations (26) and (27) for different values of p (see text for details).

p	T_{RSB}	q_{RSB}	T_G	q_G	T_G/T_{RSB}	q_G/q_{RSB}
3	1	0	1	0	—	—
4	1	0	1	0	—	—
5	1.0091	0.130	1.0100	0.0985	1.001	0.757
7	1.053	0.308	1.058	0.231	1.004	0.75
10	1.1312	0.452	1.142	0.328	1.009	0.725
20	1.364	0.641	1.393	0.468	1.02	0.73
40	1.711	0.752	1.765	0.551	1.03	0.732
100	2.388	0.838	2.496	0.633	1.045	0.755
10^3	6.075	0.931	6.51	0.721	1.07	0.774
10^4	16.54	0.966	18.05	0.769	1.091	0.796
10^5	46.69	0.981	51.64	0.802	1.1	0.817
10^6	134.65	0.989	150.5	0.835	1.12	0.844

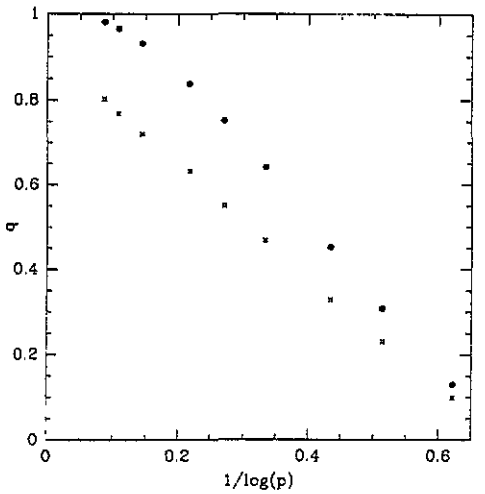

Figure 3. The static and the dynamic Edwards–Anderson parameter as a function of $1/\log(p)$. They increase logarithmically with p. The dots are for the static value, the crosses for the dynamical one.

it difficult to discern one from the other in numerical simulations. This proximity of the static and the dynamic transition temperatures is probably related to the small value of the dynamical order parameter q_G for large values of p. From these results we expect the glassy behaviour of the Potts glass to be very different from other disordered spin-glass models.

For instance, in the case of the p-spin interaction spin-glass model we have also solved the equations corresponding to (26) and (27). We have found that both the static order parameter q_{RSB} and the dynamical q_G converge to 1 in the limit $p \to \infty$ much faster than the Potts case, in agreement with theoretical expansions around the $p \to \infty$ limit [25]. For $p = 3$ (the smallest value of p compatible with a discontinuous transition) one finds in the p-spin model that

$$\begin{aligned} q_{RSB} &\simeq 0.81 \qquad (T_{RSB} \simeq 0.65) \\ q_G &\simeq 0.68 \qquad (T_G \simeq 0.68)\,. \end{aligned} \tag{31}$$

For this particular model, the ratio q_G/q_{RSB} tends to 1 in the limit $p \to \infty$ and the

ratio T_G/T_{RSB} increases with p much faster than the Potts model does (for $p = 10$ we find $q_G/q_{RSB} \simeq 0.97$ and $T_G/T_{RSB} \simeq 1.38$)

In the next section we shall compare all these predictions with Monte Carlo numerical simulations. We will see that the Potts glass transition is always present but it is far from being a complete thermodynamic freezing as happens in models where frustration is stronger (see, for instance the random orthogonal model [2]). Before showing our Monte Carlo results for the spin-glass transition it will be interesting to present some results on the ferromagnetic ordering that takes place in the Potts glass.

4. Monte Carlo tests of the glass transition

In order to simulate the Potts glass we have considered the Hamiltonian

$$\mathcal{H} = -\sum_{i<j} J_{ij}(p\delta_{\sigma_i\sigma_j} - 1) \tag{32}$$

The J_{ij} are distributed with mean J_0/N and variance equal to $\frac{1}{N}$. The only difference between the Hamiltonians of (32) and (1) is a constant which vanishes in the thermodynamic limit. We have chosen this second version because we have found that the addition of the constant strongly reduces the sample to sample fluctuations in the high-T region. This should not make too much difference for small values of p but is crucial for large values of p. All simulations implement the Metropolis algorithm with random updating.

The results we present in the next subsections correspond to annealings in which we compute the main thermodynamic observables. Starting from the high-temperature region the temperature is progressively decreased. Data are collected at each temperature and the time we stay at each temperature is the same for all temperatures during the cooling procedure. We have computed the internal energy, the magnetization of the different p-states and the associated dissipative quantities, i.e. the specific heat and the p different magnetic susceptibilities corresponding to each one of the p-states. The specific heat and the magnetic susceptibility of one of the p states is computed by measuring the fluctuations of the internal energy and the magnetization (see (7)) respectively. Typically we performed several thousands of Monte Carlo sweeps at each temperature. We draw to the attention of the reader that our results are dependent on the time schedule of the annealing only for very large values of p (i.e. where the finite-size corrections are large). Otherwise, one cannot observe a sensible dependence of the different quantities on the time the system stays at each temperature during the cooling procedure. At least, this dependence is of the same order as that arising from the sample-to-sample fluctuation. We will mainly show plots for the internal energy as a function of temperature. In all cases the Monte Carlo error bars are very small (relative error less than 10%) and will not be shown explicitly.

4.1. Ferromagnetic ordering with $J_0 = 0$

When $J_0 = 0$ the system orders ferromagnetically. We have investigated the ferromagnetic ordering for $p = 10$. This value of p is in the regime ($p > 4$) where the ferromagnetic transition is expected to appear at a temperature higher than the spin-glass transition. From (9) we expect the ferromagnetic transition to occur at $T_F = 2$. Figure 4 shows the internal energy as a function of the temperature compared to the energy of the spin-glass phase and the high-temperature result (13) for a large size $N = 1000$. The energy is lower than that corresponding to the spin-glass solution. Looking at figure 4 we observe a small jump of the energy at T close to $T_F = 2$ and that the energy is lower than the

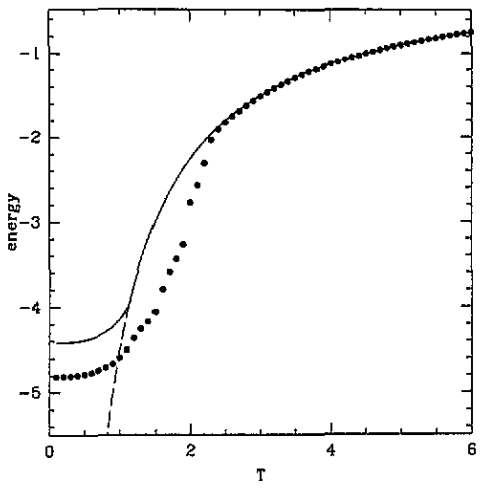

Figure 4. Energy versus temperature for the case $p = 10$ with $J_0 = 0$ and Gaussian couplings. The continuous line corresponds to the one step spin-glass solution and the dashed line is the high-T result. The ferromagnetic transition is at $T_F = 2$. Simulation results are for one sample and $N = 1000$.

high-T result already close but above $T_F = 2$. This is because above $T_F = 2$ some states begin to be strongly magnetized and this makes the energy to decrease. The specific heat also shows a peak at that temperature. This suggest the transition is first order, a natural result for a ferromagnetic transition in a Potts model which is in agreement with the mean-field equations (see [20]). To stregthen this conclusion one should perform a finite-size scaling analysis for different sizes in order to show that there is a finite jump in some dissipative magnitudes like the specific heat and the magnetic susceptibility. As a test, we have measured the magnetic susceptibility per site averaged over the different $p = 10$ states for different system sizes $N = 50, 100, 500, 1000$. We have not seen evidence for a divergence as we expect for a first order transition but a discontinuity.

It is interesting to note we have observed the emergence of further peaks at lower temperatures below T_F in the magnetic susceptibility. We interpret them as the emergence of new states which start to be macroscopically populated. These could be a sign of new transitions in the ferromagnetic phase but it is difficult to reach definite conclusions in this low-T regime.

We have also studied the zero-temperature ground state following a steepest descent procedure. We have searched for stable configurations against *one-spin* flip operations. Starting from a random initial configuration we sequentially move on the lattice selecting (among the $p-1$ possibilities) the state of the variable $\sigma(i)$ which releases the largest amount of energy. In this way the system reaches a metastable state that should be magnetized if the ground state is ferromagnetic. We have repeated this procedure several times saving the energy and the magnetization of the final configurations. Figures 5 and 6 show the distribution probability of the energies and the magnetization (7) of the stable configurations against *one-spin* flip movings for the same model $J_0 = 0$, $p = 10$ with $N = 100$. Figure 5 shows that the energies of this class of metastable states are distributed very similarly to the form predicted for the SK model [29]. This is a consequence of the glassy nature of the ferromagnetic phase. We have verified that the minimum energy found by the algorithm is higher than the energy obtained doing a slow cooling starting from the high-temperature phase. This is a proof of the glassy nature of this phase. The ferromagnetic nature (but glassy) of the phase is explicitly shown in figure 6. The value of m ranges from $m = -1$ to $m = p-1 = 9$ and the magnetization histogram shows a broad distribution between $m = -1$ and $m = 2$. The peak at $m = -1$ is consequence of the fact that only some of the $p = 10$ states are populated.

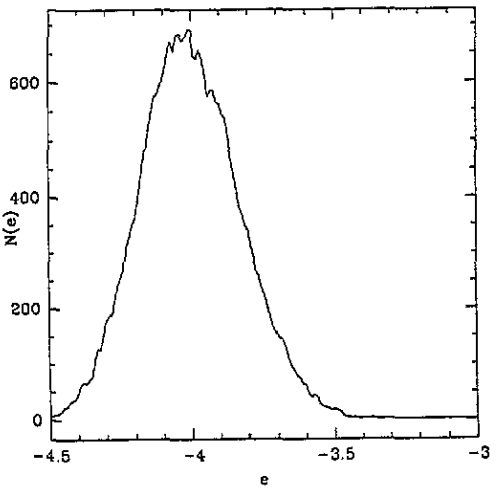

Figure 5. Probability distribution of the energy of the ground states for the case $p = 10$ and $J_0 = 0$ and $N = 100$.

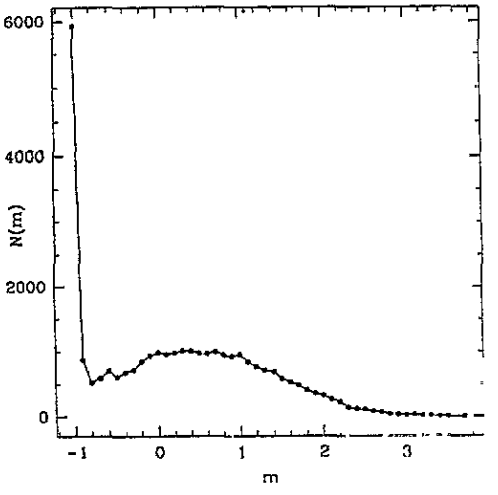

Figure 6. Probability distribution of the magnetization associated with the zero-temperature metastable states. The singularity at $m = -1$ means that only some states are populated. Parameters are as in figure 6.

4.2. The continuous transition ($p = 3$)

The case $p = 3$ is indeed very similar to the SK model ($p = 2$). Because the transition is continuous the system relaxes very close to the true energy. As mentioned in section 2, it now suffices to take $J_0 = 0$. In this way the ferromagnetic transition lies well below the spin-glass transition. In fact, we have not observed any tendency of the system to be magnetized at low temperatures. Figure 7 shows the internal energy as a function of the temperature along with the one-step solution and the high-temperature result (13). Below the critical temperature $T_{RSB} = 1$ the data departs from the prediction. Precisely at $T = 1$ the heat and the magnetic susceptibility have a cusp. Similar results for the internal energy were obtained for $p = 4$.

4.3. The discontinuous transition

To investigate the discontinuous spin-glass transition we have chosen $J_0 = \frac{1}{2}(4 - p)$ for $p > 4$. In this way the system first enters the metastable glassy phase in which there is no ferromagnetic ordering. In all our simulations we have observed that this is what happens and that there is no tendency for the ferromagnetic domains to grow as the temperature is decreased. At high temperatures the size of the domains (i.e. the fraction of sites of the lattice which are in the same state) is $1/p$. This is true down to very low temperatures where in the worst case the size of the domains increase approximately ten percent. To make any tendency to the ferromagnetic ordering completely dissapear we can increase the intensity of the antiferromagnetic coupling. This is only possible if p is not too large because otherwise finite-size corrections (an consequently finite-time effects) considerably increase. In the regime of large values of p one can neglect finite-size effects only if $p \ll N$. This is a problem of the simulations in the large-p regime. We follow the criteria for dividing our results for the discontinuous transition in two parts, the small and large

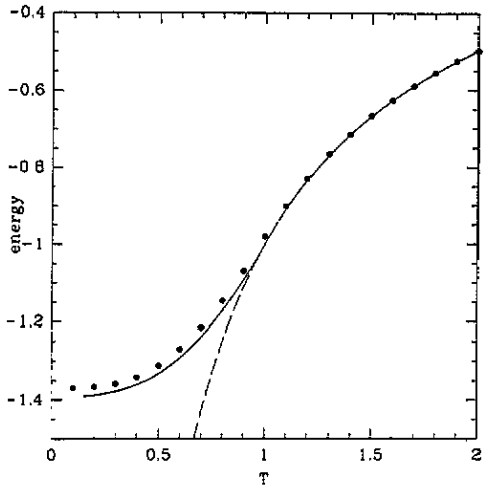

Figure 7. Energy versus temperature in the case $p = 3$, $J_0 = 0$. The continuous line is the one-step solution. The dashed line is the high-T result. The transition temperature is $T_{RSB} = T_G = 1$. The full dots are for one sample and $N = 2000$.

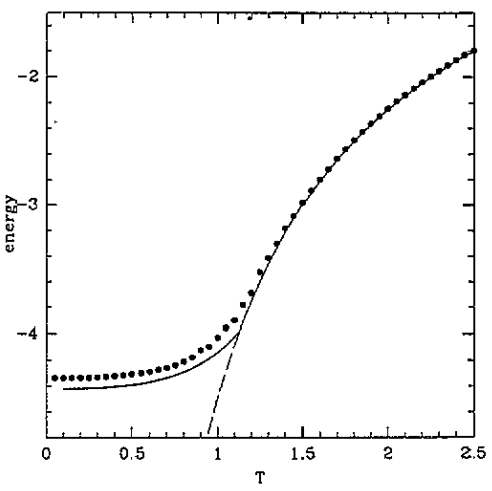

Figure 8. Energy versus temperature in the case $p = 10$, $J_0 = -3$. The continuous line is the one-step solution. The dashed line is the high-T result. The full dots are simulation results for $N = 1000$.

$p > 4$-regimes (corresponding to the regions where the finite-size corrections are expected to be small and large, respectively). It is important to note that the true distinction between the small and the large p-regime is defined by the ratio T_G/T_{RSB} or the Edwards–Anderson parameter q_G. Both parameters increase logarithmically with p. For the reasonable values of p we are able to simulate we cannot expect to observe, in the Potts glass, the region where there is a nitid glass transition. Consequently, in the next results we present, the dynamical energy departs from the high-T behaviour at a temperature higher than the glass transition temperature. This occurs because the static and the glass transition temperatures are very close to each other. We will return to this point in the conclusion.

4.3.1. The small $p > 4$-regime. We have measured the internal energy as a function of the temperature for the cases $p = 5, 10$ using a binary distribution of couplings. In this regime we have observed that the results do not vary too much depending with the time schedule of the cooling procedure. Comparison with theory is shown in figure 8 for the case $p = 10$. For these small values of p the dynamical transition practically coincides with the static one. Comparing to the previous continuous case $p = 3$ we see that the energy in the low T region for $p = 10$ remains slightly above the expected theoretical one. This is the glassy phase where the system remains trapped making excursions between several metastable states of similar energy but without reaching the static phase of slightly lower free energy. The difference in free energy (and energy) between the static phase and the metastable glassy phase is small for $p = 5$ and increases with p. It is important to note that the energy we are measuring is purely dynamical. For $p \leqslant 4$ this difference of free energy does not exist. This does not mean that the system relaxes to the true ground-state energy in an annealing process (see figure 7). In fact, for a continuous transition we expect the system should relax to the static free energy at a finite temperature very slowly (as a power

law) very similarly to the relaxation of the remanent energy or the remanent magnetisation in the SK model [30,31]. For a discontinuous transition the relaxation of the free energy takes place also very slowly but to a dynamical value higher than that predicted by the static approach. We have also computed the specific heat and the magnetic susceptibility. They display a cusp located approximately at the static transition (and, because of its proximity, near the dynamical transition also).

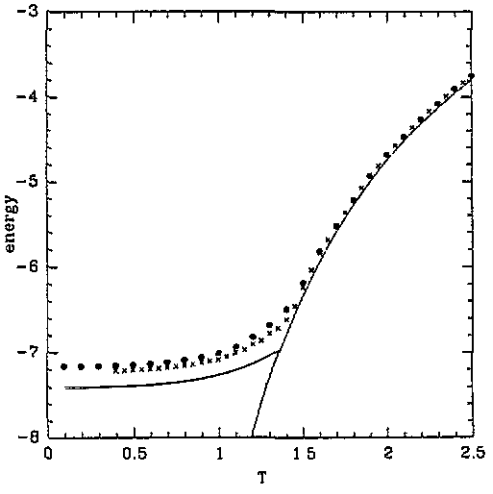

Figure 9. Energy versus temperature in the case $p = 20$, $J_0 = -8$. The continuous line is the one-step solution. The dashed line is the high-T result. The crosses and the full dots correspond to the Gaussian model with $N = 2000$ and two cooling procedures (the simulations with crosses are 10 times larger in simulation time than the dots).

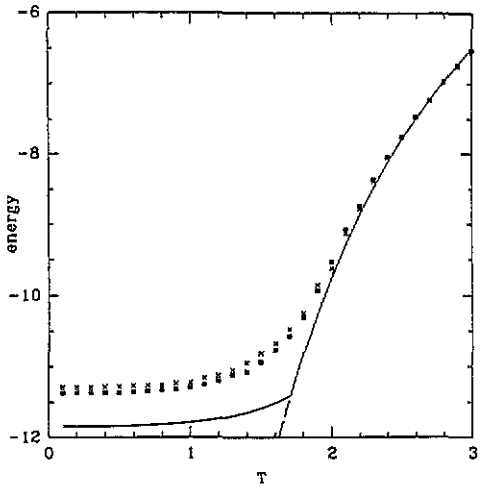

Figure 10. Energy versus temperature in the case $p = 40$, $J_0 = -18$. The continuous line is the one-step solution. The dashed line is the high-T result. The crosses and the full squares correspond to the Gaussian model with $N = 1000$ and two different samples.

4.3.2. The large $p > 4$-regime. Finite-size corrections are important and one has to simulate large sizes in order to reduce these effects. We present the results of annealings for $p = 20, 40$ in figures 9 and 10. We decided to simulate the Gaussian J_{ij} model instead of the binary $\pm J$ one in order to reduce finite-size corrections. As p increases the finite-time effects also increase and we have found a clear dependence of our results on the cooling procedure. Figure 10 shows simulation results for $p = 20$ for $N = 2000$ and two different cooling procedures. The simulation results show a drift with the annealing time. For $p = 40$ (figure 10) we show simulations of two different sample realizations. Since sample to sample fluctuations increase with p, the relative magnitude of the fluctuations of figure 10 should be considered as an upper bound for the previous figures with smaller values of p. Also finite-time effects are large for $p = 40$.

Glassy effects are slightly more pronounced in the large p-regime, the dynamical energy being larger than the static one. All dissipative quantities show a cusp very close to the dynamical transition. Even though the static and the glass transition are very close one to the other the fact that the energy of the sytem is much higher than the static one (when approaching the glass transition) is a proof that the system has entered the glassy phase.

5. Conclusions

We have studied the glassy behaviour of the mean-field Potts glass. We have been able to solve numerically the static equations at first order of replica symmetry breaking. We have also introduced a simple method, already observed by Cwilich and Kirkpatrick [22], which allows a full computation of the static and the dynamical or glass transition and the associated Edwards–Anderson parameter.

We have computed numerically the parameters of the transition for different values of p. We observe that the Edwards–Anderson parameter at the glass transition q_G increases logarithmically with p. The ratio of the static and glass temperature is smaller than 1.13 up to $p = 10^6$. The situation is very different from other disordered models such as the p-spin Ising model. For that model the dynamic transition temperature is much higher than the static one.

All our numerical results seem to indicate that the dynamical transition takes place at a temperature higher than that predicted by the theory. But this is due to the proximity of the dynamical transition to the static one. If the dynamical transition temperature were much larger than the static one then we would expect that the energy departs from the high-T result precisely at the dynamical temperature. We would expect this if we were able to simulate the Potts model with exponentially large p values. This is indeed the situation one observes in low autocorrelation models [1, 3, 7] , in the random orthogonal model [2, 6] and discrete matrix models [5] .

For large values of p (like $p = 20, 40$) we have observed a clear dependence on the time spent during the cooling procedure. The origin of the finite-time effects is related to the finite-size effects we also observe in this regime. We expect that simulations for larger sizes should give results nearly independent of the annealing time leaving only a small thermalization time effect close to the glass transition where critical effects begin to be important. We interpret this effect in the following scenario.

There are two characteristic relaxation times in the system. The first time τ_G diverges as the dynamical transition is approached, the other one τ_s diverges as the static transition is approached. Because T_G is so close to T_{RSB} the systems feels the static low-temperature phase very close to the dynamical transition temperature. Above the glass temperature we have $\tau_G \sim \tau_s$ which is certainly large if the system is entering the low-temperature phase. Because the characteristic time scale τ_G increases very fast only very close to the dynamical transition temperature then we expect that close to T_G the correlation time τ_s will set the characteristic time scale above which our simulation results should be time independent. Only for times larger than τ_s (which we are not able to reach in our simulations) the system would behave as dynamics predicts. It is then clear that all our simulation results are smeared by the static relaxation time τ_s. In the other models mentioned in the previous paragraph the dynamical transition temperature is much larger than the static one. Approaching the dynamical transition the system is in the high-temperature phase where the relaxation time is very small. Consequently, τ_G grows very much only very close to T_G (very probably diverges like $\tau_G \sim (T - T_G)^{-\gamma}$ where $\gamma = 2$ the typical value for mean-field models [7]) and the system departs from the high-T result very close to that temperature.

Because the Potts model is only partially frozen at the glass transition this is a model appropiate for study of the dynamics in the metastable glassy phase. We expect the mean-field Potts glass model to resemble real structural glasses where activated transport at the glass transition is not completely suppressed due to droplet excitations [12]. Other mean-field models without disorder freeze quickly at the glass transition and relaxation processes are strongly suppressed. In this case, much more involved numerical techniques are needed

in order to allow the system to change state and relax [32].

We would also like to emphasize that research into glassy behaviour in the presence of ferromagnetic ordering remains an interesting open problem.

Acknowledgments

We are grateful to M Campellone and E Marinari for fruitful discussions and D Lancaster for a careful reading of the manuscript. FR has been supported by the INFN.

References

[1] Marinari E, Parisi G and Ritort F 1994 Replica field theory for deterministic models: binary sequences with low autocorrelation *J. Phys. A: Math. Gen.* **27** 7615

[2] Marinari E, Parisi G and Ritort F 1994 Replica field theory for deterministic models (II): A non-random spin glass with glassy behaviour *J. Phys. A: Math. Gen.* **27** 7647

[3] Bouchaud J P and Mezard M 1994 Self-induced quenched disorder: a model for the glass transition *J. Physique I* **4** 1109

[4] Franz S and Hertz J 1994 Glassy dynamical transition and aging in a model without disorder *Preprint* cond-mat/9408079

[5] Cugliandolo L F, Kurchan J, Parisi G and Ritort F 1995 Matrix models as solvable glass models *Phys. Rev. Lett.* **74** 1012

[6] Marinari E, Parisi G and Ritort F 1995 Fully frustrated hypercubic lattices are glassy and aging at large *D* *J. Phys. A: Math. Gen.* **28** 327

[7] Migliorini G and Ritort F 1994 Dynamical behaviour of low autocorrelation models *J. Phys. A: Math. Gen.* **27** 7669

[8] Kirkpatrick S and Sherrington D 1978 Infinite-ranged models of spin glasses *Phys. Rev.* B **17** 4384

[9] Gardner E 1985 Spin glasses with *p*-spin interactions *Nucl. Phys.* B **257** 747

[10] Parisi G 1980 The order parameter for spin glasses: a function on the interval 0-1 *J. Phys. A: Math. Gen.* **13** 1101

[11] Kirkpatrick T R and Thirumalai D 1987 *p*-spin interaction spin-glass models: connections with the structural glass problem *Phys. Rev.* B **36** 5388

[12] Kirkpatrick T R and Wolynes P G 1987 Stable and metastable states in the mean-field Potts and structural glasses *Phys. Rev.* B **36** 8552

[13] Kirkpatrick T R and Thirumalai D 1988 Mean-field soft-spin Potts glass model: statics and dynamics *Phys. Rev.* B **37** 5342
Thirumalai D and Kirkpatrick T R 1988 Mean-field Potts glass model: Initial condition effects on dynamics and properties of metastable states *Phys. Rev.* B **38** 4881

[14] Crisanti A, Horner H and Sommers H-J 1993 The Spherical *p*-spin interaction spin-glass model *Z. Phys.* B **92** 257

[15] Cugliandolo L F and Kurchan J 1993 Analytical solution of the off-equilibrium solution of a long range spin glass model *Phys. Rev. Lett.* **71** 173

[16] Gross D J, Kanter I and Sompolinsky H 1985 Mean-field theory of the Potts glass *Phys. Rev. Lett.* **55** 304

[17] Derrida B 1981 Random-energy model: an exactly solvable model of disordered system *Phys. Rev.* B **24** 2613

[18] Zia R K P and Wallace D J 1975 *J. Phys. A: Math. Gen.* **8** 1495

[19] Elderfield D and Sherrington D 1983 The curious case of the Potts spin glass *J. Phys. C: Solid State Phys.* **16** L497

[20] Elderfield D and Sherrington D 1983 Spin glass, ferromagnetic and mixed phases in the disordered Potts model *J. Phys. C: Solid State Phys.* **16** L971

[21] Erzan A and Lage E J S 1983 The infinte-ranged Potts spin glass model *J. Phys. C: Solid State Phys.* **16** L555

[22] Cwilich G and Kirkpatrick T R 1989 Mean-field theory and fluctuations in Potts spin glasses: I *J. Phys. A: Math. Gen.* **22** 4971

[23] For general reviews on spin glasses see:
Mézard M, Parisi G and Virasoro M A 1987 *Spin Glass Theory and Beyond* (Singapore: World Scientific)
Fischer K H and Hertz J A 1991 *Spin Glasses* (Cambridge: Cambridge University Press)
Parisi G 1992 *Field Theory, Disorder and Simulations* (Singapore: World Scientific)
Binder K and Young A P 1986 Spin glasses: experimental facts, theoretical concepts and open questions *Rev. Mod. Phys.* **58** 801
[24] Goldschmidt Y Y 1989 Exact Solution of Potts random energy Models with weak connectivity and of the many states Potts spin glass *J. Phys. A: Math. Gen.* **22** L157
[25] Campellone M *Tesi di Laurea*; Some non-perturbative calculations on spin glasses *J. Phys. A: Math. Gen.* **28** 2149
[26] The marginality condition appears in different places in the literature. Among them:
Sommers H J 1983 On the dynamic mean-field theory of spin glasses *Z. Phys.* B **50** 97
Kondor I and De Dominicis C 1986 Ultrametricity and zero modes in the short-range Ising spin glass *Europhys. Lett.* **2** 617
Horner H 1980 *Z. Phys.* B **80** 95
[27] Brunetti R, Parisi G and Ritort F 1992 Asymmetric little spin-glass model *Phys. Rev.* B **46** 5339
[28] Gross D J and Mezard M 1984 The simplest spin glass *Nucl. Phys.* B **240** 431
[29] Bray A J and Moore M A 1980 Metastable states in spin glasses *J. Phys. C: Solid State Phys.* **13** L469
[30] Parisi G and Ritort F 1993 The remanent magnetization in spin glass models *J. Physique I* **3** 969
[31] Ferraro G 1994 Infinite volume relaxation in the Sherrington–Kirkpatrick model *Preprint* cond-mat/9407091
[32] Krauth W and Mezard M 1994 Aging without disorder on long time scales *Preprint* cond-mat/9407029
Krauth W and Pluchery O 1994 A rapid dynamical Monte Carlo algoritm for glassy systems *Preprint* cond-mat/9407017